Accepted manuscript doi:
10.1680/jgeen.18.00178

Accepted manuscript doi:
10.1680/jgeen.18.00178

Submitted: 25 September 2018

Published online in 'accepted manuscript' format: 19 February 2019

Manuscript title: The impact of the Crossrail tunnelling project on masonry buildings with shallow foundations

Authors: Matthew J. DeJong[1], Giorgia Giardina[2], Benjamin Chalmers[3], Deborah Lazarus[4], David Ashworth[5] and Robert J. Mair[6]

Affiliations: [1]Department of Civil and Environmental Engineering, University of California, Berkeley, USA; [2]Department of Architecture and Civil Engineering, University of Bath, UK; [3]Laing O'Rourke; [4]Arup; [5]Atkins, Member of the SNC-Lavalin Group and [6]Department of Engineering, University of Cambridge

Corresponding author: Giorgia Giardina, Department of Architecture and Civil Engineering, University of Bath, UK.

E-mail: g.giardina@bath.ac.uk

Accepted manuscript doi:
10.1680/jgeen.18.00178

Abstract

Building monitoring and protection are important components of underground projects in urban areas. Typically applied procedures for the assessment of settlement-induced damage to buildings are based on simplified assumptions that do not take into account soil-structure interaction. Assessment methods based on the relative stiffness between the structure and the soil exist, but they are rarely applied in practice due to concerns about the accuracy and reliability. The primary aim of this work is to use the large amount of monitoring data provided by the Crossrail project in London to improve understanding of building performance and existing damage assessment methods. The paper gives an initial overview of the available monitoring data by presenting four representative case studies for loadbearing masonry buildings on shallow foundations. Structural data is then used to evaluate the consistency of predictions produced by different relative stiffness formulations. The results show the effect of building stiffness on the soil surface settlements and clarify the effects of various assumptions made during prediction. The conclusions highlight opportunities to improve prediction procedures and the need for more detailed monitoring data for future tunnelling projects.

Keywords: damage assessment; greenfield movements; loadbearing masonry; relative stiffness; bore tunnelling

Accepted manuscript doi:
10.1680/jgeen.18.00178

1 Introduction

Crossrail is currently the biggest railway construction project in Europe. In the central London section, the excavation works potentially affect a large number of buildings along the route of construction. More than 1200 buildings required an initial vulnerability assessment against the possible damage caused by the tunnelling-induced settlements (Torp-Petersen & Black, 2001). The work associated with protecting structures (surveys, assessments, monitoring and intervention works) along the route of construction was a significant proportion of the total project costs. These numbers highlight the importance of damage assessment procedures able to give a conservative, rapid, consistent and reasonably accurate estimation of tunnelling-induced effects on buildings.

Predictions of damage to the many buildings (and other assets) along the Crossrail alignment were made using the methodology set out in Crossrail Information Paper D12 Ground Settlement (Crossrail, 2008). This built on the experience of recent tunnelling projects in London, notably the Jubilee Line Extension and High Speed 1. This method uses conservative assumptions; in particular the effect of the structure on soil displacements is not taken into account and settlements are assumed to follow a Gaussian trough, known as the greenfield settlements (Peck, 1969).

Several alternative methods have been developed to consider the soil-structure interaction by calculating the relative stiffness of the structure with respect to the soil stiffness (Potts & Addenbrooke, 1997; Son & Cording, 2005; Franzius et al., 2006; Goh & Mair, 2011); these methods are not currently used when assessing structures due to concerns about the potential effect of uncertainties on the predicted damage. Large scale and extensively monitored projects like Crossrail are a precious source of information on real building response to tunnelling and deep excavations (e.g. Burland et al. (2001)). This information can be used to deepen the understanding of the interaction between the soil and the buildings, and to verify and improve the existing assessment methods.

The aim of this paper is to summarise the lessons learned from Crossrail with regards to building performance and suitability of damage assessment procedures. First, the type of data made available by the project is illustrated by describing four case studies. Then the specific building information is used to evaluate the consistency of available damage assessment methods that take into account soil-structure interaction. Both of these contributions provide new information that can be used to improve the robustness and accuracy of current methods, which would benefit future underground projects in urban areas.

2 Building monitoring

Prior to the excavation, extensive monitoring instrumentation was installed route-wide on the ground, tunnels and individual assets. In particular, three major types of measuring points were installed: 3D reflective prisms, precise levelling points (PLP) and levelling points installed on structures using BRE sockets.

This section presents the monitored displacements of four buildings along the Western Drive (Paddington - Farringdon). This part of the tunnelling route is constructed in London Clay. Details on geological sections along the entire Crossrail route can be found in Black (2017). The structures were chosen among masonry buildings on shallow foundations that were located along the bored tunnels in areas where ground movements were not influenced by shaft or station box excavations, or by the construction of SCL tunnels. Focus was placed on buildings which were oriented approximately perpendicular to the tunnel axis; a minimum

Accepted manuscript doi:
10.1680/jgeen.18.00178

angle of 75 degrees between the tunnel axis and the orientation of the longest dimension of the building in plan was specified as the orientation criterion.

Initially, 26 listed masonry buildings along the Crossrail Western Drive were identified. Based on Crossrail's assessments, negligible damage was predicted for the selected structures. The case study search was therefore expanded to include non-listed buildings that had a higher damage prediction based on the greenfield ground movements. In this way, the number of selected structures was increased to 54. It should be noted that this figure does not correspond to the number of assets in the Crossrail database due to a difference in the definition of what constitutes an individual structure between this study and Crossrail. For the former, for example, one continuous terrace of buildings is counted as one structure, whereas in the Crossrail database this may be included as a number of different assets corresponding to separate postal addresses or ownership.

The results presented in the next sections refer to four out of the 54 buildings that were analysed. These four had the most structural monitoring data available. For each case study, a 2D plan and transect of the structure, tunnels and monitoring points were produced. Crossrail used the London Survey Grid defined by London Underground. The coordinates of the structure were identified using Ordinance Survey mapping; the identified OS coordinates were converted to the London survey grid using the transformation defined in London Underground standard 1-026 Topographical Surveys and Mapping (London Underground, 2011).

The effect of the structure on the greenfield settlements was highlighted by comparing the limited BRE and prism data to the PLP transects, which represent the greenfield scenario. In a major city such as London, there are not many open spaces, so a significant number of PLP transects were installed in the pavement. As the zone of influence of a structure parallel to the tunnel axis is not well defined, it is possible that these transects measure settlements that are somewhere between true greenfield settlements and the settlement experienced by the structure. To allow consideration of this effect, the different PLP transects are separated in the figures, and the outline of the nearby structures included.

For each analysed building, the theoretical greenfield settlement profile that was used for the preliminary Crossrail damage assessment is presented. This settlement profile, labelled as "predicted greenfield", was calculated by using a Gaussian approximation (Peck, 1969) with assumed volume loss $V_L = 1\%$, trough width parameter $k = 0.5$ and actual tunnel depth z_0 at the corresponding section. Furthermore, a Gaussian curve with the same k and z_0 values and reproducing more closely the monitored displacements ("actual greenfield") was added for comparison. This allowed better estimation of the actual volume loss and better evaluation of the measured settlement profile compared to a greenfield profile.

2.1 129-133 Park Lane

Park Lane is situated on the boundary of Hyde Park (Figure 1). The row of houses including 129-133 Park Lane will be considered as a single connected building (Figure 2a), which is located on the east side of Park Lane and includes the addresses on 22 Dunraven Street behind. The building is constructed of load-bearing masonry and comprises four floors and a single basement from the original construction c1757-8, with later extensions including attic floors which were added in the 19th century. They are assumed to have shallow ground-bearing foundations consistent with their age of construction.

Figure 3a shows the locations where vertical displacements were monitored in the vicinity of the building comprising 129-133 Park Lane. Since the area to the west of the structure is undeveloped, PLP Transect 1 is affected only by this structure and the structure across the

Accepted manuscript doi:
10.1680/jgeen.18.00178

street to the south (Figure 2). There are three prisms mounted onto the structure on the opposite face to the PLP transect (the Dunraven Street side of the building). Limited structural information was available, namely only the external dimensions and an estimate of percentage of openings. The westbound tunnel was bored first, followed by the eastbound tunnel.

Figure 3b shows the vertical settlements projected onto the transect line depicted in Figure 3a. The plotted data for PLP transects 1 and 2 were taken well after the tunnel passed. The settlements observed at the three BRE points on the structure compare well with PLP transect 1, and PLP transects 1 and 2 also compare well with each other. The plotted data for PLP transect 3 are the last measurements recorded, which were taken while the westbound tunnel was passing beneath the structure. Thus, the magnitude of the displacement is smaller, since westbound tunnelling was still in progress and the eastbound tunnel had yet to be bored, and the variation in vertical displacement along the axis of the tunnel is expected due to the transient differential settlement in the longitudinal direction.

The greenfield settlement prediction for 1% volume loss for both tunnels is shown to over-predict all monitoring data. The closer Gaussian curves ("actual greenfield") would give a volume loss of 0.7%. The three prism points installed on the building under consideration (129-133 Park Lane) suggest that the structure is in hogging, as predicted by the greenfield profile and measured by PLP transect 1. However, the three points are not sufficient to confirm where the distortions of the structure begin or to quantify the deflection ratio. Thus, the data is not detailed enough to further evaluate the effect of the building on the settlement profile, but it is possible that the stiffness of the structure reduced the distortion of the building.

Furthermore, the PLP transect 1 data appears flat beneath the building, indicating a larger settlement than the greenfield prediction at further distances from the tunnel axis, and smaller settlement than the greenfield prediction closer to the tunnel axis. This could potentially indicate some influence from the building on the PLP data. Similarly, the PLP Transect 1 data was recorded much closer to Avenfield House (Figure 2b), which is the dashed building in Figure 3a that is just south of 129-133 Park Lane. In this case, the evidence that the building influenced the PLP transect 1 settlements is stronger. The building appears to have embedded at its north end, just above the eastbound tunnel, and significantly reduced the curvature of the settlement profile compared to the greenfield prediction. This is expected as the building is relatively stiff, but it also further highlights the challenge of determining whether the PLP transects are influenced by adjacent structure.

2.2 6-14 Bedford Row

The Georgian building at 6-14 Bedford Row is comprised of a terrace of 1717-18 townhouses by Robert Burford, all of which have many common elements and form a significant historic streetscape. The building is broadly aligned transverse to the running tunnels (Figure 4).The houses are Grade 2* listed. The terrace is four storeys plus a basement and an attic. The front and rear facades are constructed from brown brick and have tall windows (Figure 5). The terrace is load bearing brick masonry construction founded on corbelled brick footings, set at a shallow depth below the basement floors.

Figure 6 shows the locations where monitoring data was collected, and the final settlement data after tunnelling was complete, again projected on to the transect line. The three PLP transects running parallel to the structure in nearby footways correspond well to each other with no systematic variation between them. Bedford Row is situated in an area where relatively high volume loss occurred, and the PLP transects compare well with the 1%

Accepted manuscript doi:
10.1680/jgeen.18.00178

volume loss greenfield prediction. Further, the three BRE points installed towards the southern end of the structure also correspond well to the PLP transects. It could be reasonably assumed that the rest of the structure would also follow the PLP transect, although more monitoring points along the structure would be required to confirm this. If this were the case, the data suggests that the structure is relatively flexible and did not alter the expected greenfield settlements significantly. It should also be noted that 6-14 Bedford Row belongs to a longer building terrace. The extent of the selected building approximately corresponds with the 1 mm settlement limit (Figure 4).

2.3 172-184 Shaftesbury Avenue

The terrace properties 172-184 Shaftesbury Avenue form a triangular building that lies above the eastbound tunnel (Figure 7). It comprises two smaller properties and Shaftesbury Hospital (172-176), which extends through to Monmouth Street behind. The buildings have a basement, and the hospital has five storeys above ground while the surrounding buildings have four storeys (Figure 8). The buildings are load bearing masonry and date from pre-1900. The Hospital opened in 1867 and was converted to a hotel sometime after 1992 when it closed as a medical facility. As for Bedford Row, the analysed buildings are approximately defined by the 1 mm settlement line.

Figure 9 shows the monitoring locations and the vertical settlements, again projected on the transect line perpendicular to the tunnel, measured after tunnelling was complete. The vertical settlement trough can be approximated by a Gaussian curve with $V_L = 0.55\%$. The buildings on Shaftesbury Avenue are only affected by the eastbound tunnel, due to the increased separation of the tunnels in this area. There are two PLP transects, one on either side of the building, which correspond well to each other. The PLP transects suggest that the trough width is increased compared to the original predictions produced by Crossrail; the increase in trough width could either be caused by variations in the soil properties or the effect of the building stiffness. Again, the PLP transects run on the pavement adjacent to the structure, so the influence of the building on the PLP transects is difficult to determine, making it harder to interpret the results.

2.4 38-44 Berwick Street

The terrace of properties on the east side of Berwick Street (Figure 10) dates from pre-1900 with later additions and alterations. The properties are three to five storeys (see Figure 11), and have a single level of basement.

Figure 12 shows the monitoring locations and the vertical settlements, again projected on the transect line perpendicular to the tunnel, and measured after tunnelling was complete. The Gaussian curve approximating the vertical settlements corresponds to a volume loss of 0.55%. The separation of the tunnels at this location results in 3 hogging zones and 2 sagging zones; the middle hogging zone has the potential to have a large deflection ratio and therefore a high level of damage. There are two PLP transects parallel to the structure and one transect perpendicular to the structure (Figure 12).

There are five monitoring points installed on the structure covering most of the building length. The two parallel transects differ considerably. PLP Transect 1 data was taken on the pavement in front of the buildings on Berwick Street, and agrees well with the BRE points on the adjacent structure. This indicates that the PLP data was probably affected by the building, though the extent of influence cannot be determined without additional monitoring data further away from the building. Both the PLP transect and building monitoring data suggests

Accepted manuscript doi:
10.1680/jgeen.18.00178

that the volume loss was less than 1% , and that the deflection ratios in the sagging zones and central hogging zones were reduced compared to greenfield predictions.
Remarkably, PLP Transect 1 appears similar to the greenfield, though partially "smoothed" by the stiffness of the buildings. On the other hand, PLP Transect 2 data, which was collected on Wardour Street (see Figure 10), indicates a settlement profile which seems to have been more influenced by adjacent buildings. More specifically, the building on the west side of Wardour Street appears to have been relatively rigid, and seems to have rotated towards the south-west causing some embedment at the D'Arblay Street intersection. Points on this building were not monitored directly, so could not be compared with PLP Transect 2 data, but this gives strong evidence the PLP data is significantly influenced by the relative stiffness of the adjacent building. It is noteworthy that the building at 167-169 Wardour Street, adjacent to PLP transect 2, is a predominantly 5-storey building, much of which was originally built as one building (see Figure 13). It is not surprising that this structure appears to have behaved more rigidly than the terrace on Berwick Street.

2.5 Discussion

For the Crossrail project, extensive instrumentation was installed route-wide to monitor the displacements of the ground and surface buildings. Ideally, this data would offer the possibility to evaluate the effect of buildings on tunnelling-induced settlements by comparing the displacements measured on free field transects with the building movements. Toward this objective, the case studies above are an attempt to interpret the available data, but the limitations of the data are clear. The number of monitoring points on buildings was not sufficient to directly determine an accurate settlement profile of the structure itself, and there is uncertainty regarding how well data from PLP transects, which are adjacent to buildings but vary in their distance away from them, should compare with movement of the building itself. In future urban underground projects of such a large scale, it would be extremely useful to take better advantage of the potential of structural monitoring data by including significantly more than three monitoring points (as generally used on Crossrail) for particular buildings of interest.
Regardless, the database of Crossrail monitoring data and building structural features was of great value to quantify and understand the ground movements along the tunnel drive, and to look further at specific case studies as demonstrated above. In the next section, the same case studies will be used to evaluate the consistency of available damage assessment methods.

3 Building damage assessment

The procedure adopted by Crossrail for the initial assessment of building damage is based on the empirical-analytical method originally developed by Burland and Wroth (1974) and summarised by Mair (1996). This procedure consists of three phases, describedin the sections below.

3.1 Phase 1

Prior to the assessment, all the structures influenced by the constructions of tunnels, shafts and stations are identified. The ground movements due to tunnel construction are calculated without taking into account the surface buildings, e.g. by using the method developed by Peck (1969). All assets within the zone of influence are assigned a unique asset ID. Based on these greenfield displacements, any structure outside the 10 mm settlement contour or located on a settlement zone with a slope less than 1/500 is deemed to require no further assessment, with all others proceeding to Phase 2 (and in some cases Phase 3 as described below).

Crossrail identified 467 buildings within the 10 mm contour and/or with predicted ground slope greater than 1/500 along the Western Drive. These structures are selected for Phase 2 assessment, unless they are listed or have piled or deep (greater than 4m depth or 20% tunnel depth) foundations, in which case Phase 3 assessment at is automatically specified. In total, 320 buildings moved to Phase 2 assessment while 147 buildings skipped directly to Phase 3 assessment.

3.2 Phase 2

The second phase of the assessment is to impose the calculated ground movements on the structures identified at Phase 1 (Limiting Tensile Strain Method, LTSM). By treating the building as a linear elastic beam and by using the deflection ratio Δ / L (Figure 14) as an indicator of the settlement-induced distortion, Burland and Wroth (1974) derived the following relationships:

$$\varepsilon_{b,\text{sag}} = \frac{\Delta}{L}\left[\left(\frac{L}{6H} + \frac{H}{4L}\frac{E}{G}\right)\right]^{-1} \tag{1}$$

$$\varepsilon_{b,\text{hog}} = \frac{\Delta}{L}\left[\left(\frac{L}{12H} + \frac{H}{2L}\frac{E}{G}\right)\right]^{-1} \tag{2}$$

$$\varepsilon_{d,\text{sag}} = \frac{\Delta}{L}\left[\left(1 + \frac{2L^2}{3H^3}\frac{G}{E}\right)\right]^{-1} \tag{3}$$

$$\varepsilon_{d,\text{hog}} = \frac{\Delta}{L}\left[\left(1 + \frac{L^2}{6H^2}\frac{G}{E}\right)\right]^{-1} \tag{4}$$

These equations relate the bending strain ε_b and the diagonal strain ε_d to the deflection ratio Δ / L, the height H, the length L and the ratio E/G between the bending and shear stiffness of the equivalent beam. The calculation of bending and diagonal strains is performed separately for the sagging and hogging part of the settlement profile (Figure 14).

The total bending and diagonal strains include the horizontal strain ε_h, according to the following expressions:

$$\varepsilon_{bt} = \varepsilon_b + \varepsilon_h \tag{5}$$

$$\varepsilon_{dt} = 0.35\varepsilon_h + \left(0.65\varepsilon_h\right)^2 + \varepsilon_d^2 \tag{6}$$

where ε_b and ε_d are the maximum of the two strains calculated in Equations 1 and 2, and 3 and 4, respectively, and ε_h is defined as the ratio between the horizontal movements at both ends of the building and the building length. The total strains are then compared to limiting values in order to define the damage category (Burland, 2012).

To avoid having to do a detailed assessment of every unique building during the Crossrail Phase 2 assessment, a set of generic structures with varying length, height and eccentricity were created at regular intervals along the transect. The generic buildings were assumed to have foundations of a negligible depth so that the greenfield surface profile could be directly

used to calculate the building strains. The real buildings were then mapped to these generic buildings to estimate the damage caused to each building. The process of converting the real buildings to the generic assessment introduces additional conservative assumptions. The assumptions for the volume loss and trough width parameter were defined as $V_L = 1\%$ and $k = 0.5$ (Crossrail, 2009). This generic assessment was used to assess all 320 buildings specified for Phase 2 assessment. None of these buildings were predicted to have a damage category of greater than 2, and consequently no further assessment was required.

3.3 Phase 3

In general, for Phase 2 assessments that result in a damage category of 3 or higher, and for all buildings that are listed or have deep/piled foundations, Phase 3 assessment is required. This is a more accurate analysis. For Crossrail, Phase 3 consisted of three stages of analysis with increasing level of detail, the results of which inform the design of remedial work where required. The first stage of this process, designated Phase 3.1, was to perform the same analysis as in Phase 2 but for each structure individually and by applying the greenfield profile at the base of the foundations. The next two stages involved using more information, including soil structure interaction, construction methodology, 3D behaviour and identification of any structural or heritage features with increased levels of risk. Most of the listed masonry buildings on the Western Drive were assessed to have a damage category of 0 or 1 after the Phase 3.1 assessment, and therefore did not require any further evaluation. According to the Crossrail documentation (Crossrail, 2008), for the structures that required Phase 3.2 and 3.3 assessment, analytical/empirical relative stiffness methods (RSMs, discussed below) were not explicitly recommended. Instead, the use of detailed computational models was suggested. The sections below outlines some of the previously proposed relative stiffness procedures, and applies them to the case studies discussed previously. The objective is to evaluate their consistency and their potential utility for future tunnelling projects.

3.4. Relative stiffness

Phase 2 assessment, as outlined above, is conservative in most scenarios, because it neglects the effect of the building stiffness on the building response. Alternatively, a relative stiffness approach can be used (e.g. Potts & Addenbrooke (1997)). This method is based on the concept of modification factors, which quantify the effect of the soil-structure interaction on the greenfield profile, and are defines as:

$$M^{DR,\mathrm{sag}} = \frac{(\Delta / L)_{sag}}{(\Delta / L)^{g}_{sag}} \tag{7}$$

$$M^{DR,\mathrm{hog}} = \frac{(\Delta / L)_{hog}}{(\Delta / L)^{g}_{hog}} \tag{8}$$

$$M^{\varepsilon_h} = \frac{\varepsilon_h}{\varepsilon^{g}_{h}} \tag{9}$$

where the deflection ratio ($M^{DR,\mathrm{sag}}, M^{DR,\mathrm{hog}}$) and horizontal strain (M^{ε_h}) modification factors are defined as the ratio between the greenfield parameters $(\Delta / L)^{g}_{\mathrm{sag}}$, $\Delta / L)^{g}_{\mathrm{hog}}$ and ε^{g}_{h} and the corresponding actual values resulting from the soil-structure interaction. Given an estimation

for the modification factors, depending on the building and soil characteristics, the predicted values for the actual deformations can be used to calculate the limiting tensile strain according to Equations 1-6.

The modification factors are calculated using design charts that are dependent on the relative stiffness between the building and the soil and the relative eccentricity of the structure with respect to the tunnel. Different formulations for the relative stiffness have been proposed. This work considers the original definition by Potts & Addenbrooke (1997) and the subsequent alterations by Franzius et al. (2006) and Goh & Mair (2011).

3.4.1. Potts & Addenbrooke (1997)

Potts & Addenbrooke (1997) defined dimensionless relative stiffness expressions for the relative bending stiffness ρ^* and relative axial stiffness α^*:

$$\rho^* = \frac{16EI}{E_s L^4} \tag{10}$$

$$\alpha^* = \frac{2EA}{E_s L} \tag{11}$$

where EI and EA are the bending and axial stiffness of the building, respectively, while E_s is the reference soil stiffness. Based on parametric finite element analyses, Potts & Addenbrooke (1997) produced design charts which relate the deflectionratio and horizontal strain modification factors with the bending and axial building stiffness.

3.4.2 Franzius et al. (2006)

Franzius et al. (2006) redefined the relative bending stiffness ρ^* and the relative axial stiffness α^* by including the tunnel depth z_0 and the building width B. In this way, he guaranteed that the two parameters would be dimensionless in both 2D and 3D:

$$\rho^*_{\text{mod}} = \frac{EI}{E_s L^2 z_0 B} \tag{12}$$

$$\alpha^*_{\text{mod}} = \frac{EA}{E_s BL} \tag{13}$$

If a plane strain model is used and the stiffness calculated per metre, then B = 1 m/m is used to maintain the non-dimensionality of the parameter.

3.4.3 Goh & Mair (2011)

Goh & Mair (2011) redefined the relative bending stiffness for the lengths L_{hog} and L_{sag} of the structure in the hogging and sagging zones, respectively, while maintaining use of the entire building length for the definition of the relative axial stiffness:

$$\rho^*_{\text{sag,par}} = \frac{EI}{E_s L^3_{sag}} \tag{14}$$

Accepted manuscript doi:
10.1680/jgeen.18.00178

$$\rho^*_{\text{hog,par}} = \frac{EI}{E_s L^3_{hog}} \tag{15}$$

$$\alpha^*_{\text{par}} = \frac{EA}{E_s L} \tag{16}$$

Goh & Mair (2011) also produced an upper and lower bound for the hogging and sagging deflection ratio modification factors.

4 Application to the case studies

For the case studies presented previously, the available information regarding the greenfield displacements and building characteristics (Table 1) was used to calculate the expected deflection ratio according to the three presented variations of the relative stiffness method. Results are reported in Table 2 and Figure15a. Figure 15b shows the comparison between the results from the Phase 2 assessment (Burland, 2012) and the RSMs, confirming the conservative tendency of the greenfield-based approach.

In general, the relatively broad scatter in the predicted modification factors emphasises the need for a more consistent procedure. However, some important trends are evident. In all cases, the Franzius et al. (2006) formulation is more conservative than the Potts & Addenbrooke (1997) formulation. The Goh & Mair (2011) lower bound is consistently smaller than any other predictions, while the upper bound is generally slightly smaller than Potts & Addenbrooke (1997) modification factors.

Looking more specifically at the results, 129-133 Park Lane was predominantly in hogging, so the hogging results are more relevant. The monitoring data for that building was inconclusive, but indicated that some modification of the greenfield settlement profile had occurred. The Potts & Addenbrooke (1997) and Goh & Mair (2011) upper bound predictions appear plausible.

For 6-14 Bedford Row, which contained significant regions of both sagging and hogging, the monitoring results were more convincing (though still not conclusive), indicating that the measured settlement in sagging matched the greenfield results well, resulting in a modification factor of approximately 1. In this case, all formulations, with the exception of the Goh & Mair (2011) lower bound provide a good prediction for sagging. For all the relative stiffness variations, taking into account the whole length of the terrace row, as opposed to only considering the portion within the 1 mm settlement line, would lead to a higher modification factor, i.e. the evaluation of the building as more flexible. In hogging, the BRE data indicates that the building may have lifted up from the ground slightly, which would have caused a modification factor of less than 1, while the PLP results again indicate a modification factor of 1. This once more exemplifies the potential difference between PLP data adjacent to buildings, and the movement of the buildings themselves.

For 172-184 Shaftesbury Avenue, the structure again spans both the hogging and sagging regions. The relatively wide trough width observed by monitoring data led to the conclusion that the building had some effect on the settlement profile. The discrete BRE monitoring data at the end of the building did indicate that the settlement profile of the building itself may have even been flatter than shown by the PLP data. In sagging, the modification factors predicted by Potts & Addenbrooke (1997), Franzius et al. (2006), and Goh & Mair (2011) upper bound seem plausible if compared to the PLP data (though the building itself could of course have behaved differently). In hogging, the data is not clear, so all predictions except the Goh & Mair (2011) lower bound result appear reasonable.

Accepted manuscript doi:
10.1680/jgeen.18.00178

Finally, for 39-44 Berwick Street, the structure spans both hogging and sagging, and the interaction of the two tunnels caused a more complicated settlement profile. In this case, the stiffness of the building seems to have had a minor effect. Generally, the modification factors predicted by Franzius et al. (2006) for hogging and Potts & Addenbrooke (1997), Franzius et al. (2006) and Goh & Mair (2011) upper bound for sagging appear reasonable, while the rest appear rather low. It should be noted that the relatively flexible response of the building compared with many of the relative stiffness method results could be due to lack of connectivity between terrace buildings, which was not evaluated. Each building within the terrace is quite different (Figure 11), particularly compared to other terraced properties or buildings which are clearly integrated (e.g. Figure 13). The connectivity of terraced buildings and foundations should be explicitly included in future developments of relative stiffness procedures.

5 Conclusions

This paper analysed the available Crossrail monitoring data to better understand the interaction between soil and surface structures due to tunnelling. The two main objectives of this work were the evaluation of the building performance and the assessment of current methodologies for the prediction of building damage.

This investigation concluded that, due to the limited number of monitoring points for each structure, it was not possible to accurately evaluate the actual building deformations with respect to the greenfield profile. However, some evidence that the building stiffness modified the ground settlement profile was clearly observed. This highlighted the difficulty in evaluating to what extent the PLP transects were affected by the stiffness of adjacent buildings; some effect was clearly observed.

Due to the absence of significant structural damage, it was also difficult to evaluate the accuracy of the damage classification obtained by using either the LTSM or the relative stiffness method. However, the case studies considered demonstrate significant variations between the predictions produced using relative stiffness formulations available. An extensive evaluation of the factors governing these variations has been presented in Giardina et al. (2018a). Some methods appear to have performed better than others, but further research and monitoring data is essential to further improve these assessment procedures.

Based on these conclusions, it is strongly recommended that more detailed building monitoring data, in addition to PLP transect data, is collected in future tunnelling projects. More specifically, denser building displacement data, in addition to direct measurement of distributed strain data (e.g. using fibre optic strain measurement), would be beneficial to further evaluate prediction methods. Alternatively, recent studies (Giardina et al., 2018b; Milillo et al., 2018) have demonstrated that Synthetic Aperture Radar Interferometry (InSAR) shows potential to augment in-situ monitoring of building deformations. This remote sensing technique provides high-resolution, day-and-night and weather independent images that can be used to monitor deformations over extensive areas, and can be applied retrospectively. As InSAR monitoring techniques continue to improve, this technique could provide data for an extensive number of buildings at a significantly reduced cost, enabling further improvement of prediction procedures.

Acknowledgements

Financial support was provided by Crossrail and by the Engineering and Physical Sciences Research Council of the United Kingdom, under Grant reference number EP/K018221/1. The research materials supporting this publication can be accessed at https://doi.org/10.15125/BATH-00583.

List of Notations

A	cross sectional area
α^*	relative axial stiffness
α^*_{mod}	modified relative axial stiffness
α^*_{par}	partitioned relative axial stiffness
Δ	deflection
Δ / L	deflection ratio
E	bending stiffness
E_s	reference soil stiffness
ε_b	bending strain
$\varepsilon_b t$	total bending strain
ε_d	diagonal strain
ε_d	total diagonal strain
ε_h	horizontal strain
g	greenfield
G	shear stiffness
hog	hogging
H	building height
I	moment of inertia
k	trough width parameter
L	building length
M^{DR}	deflection ratio modification factor
M^{ε_h}	horizontal strain modification factor
ρ^*	relative bending stiffness
ρ^*_{mod}	modified relative bending stiffness
ρ^*_{par}	partitioned relative bending stiffness
sag	sagging
V_L	volume loss
z_0	tunnel depth

References

Black, M. (2017). Crossrail project: managing geotechnical risk on London's Elizabeth line. *Proceedings of the Institution of Civil Engineers: Civil Engineering* **170**(CE5), 23–30.

Burland, J. B. (2012). *Ice manual of geotechnical engineering: Volume I.* Institution of Civil Engineering. Chap. Building response to ground movements.

Burland, J. B., Standing, J. R. & Jardine, F. M. (2001). *Building response to tunnelling: case studies from construction of the Jubilee Line Extension, London*. CIRIA Special Publication Series, London: Thomas Telford.

Crossrail (2008). *Crossrail information paper D12 – Ground Settlement*. Tech. Rept. 5th edition.

Crossrail (2009). *Civil Engineering Design Standard Part 7, Ground Movement Prediction. Crossrail Document No. CRD-STD-303-7*. Tech. rept.

Franzius, J. N., Potts, D. M. & Burland, J. B. (2006). The response of surface structures to tunnel construction. *Proc Inst Civil Eng: Geotech Eng* **159(**1), 3–17.

Giardina, G., DeJong, M., Chalmers, B., Ormond, B. & Mair, R. (2018a). A comparison of current analytical methods for predicting soil-structure interaction due to tunnelling. *Tunnelling and Underground Space Technology* **79**, 319–335.

Giardina, G., Milillo, P., DeJong, M. J., Perissin, D. & Milillo, G. (2018b). Evaluation of InSAR monitoring data for post-tunnelling settlement damage assessment. *Structural Control and Health Monitoring* , (ahead of print).

Goh, K. H. & Mair, R. J. (2011). The response of buildings to movements induced by deep excavations. *Geotechnical Engineering Journal of the SEAGS and AGSSEA* **42(**3).

London Underground (2011). *1-026 topographical surveys and mapping*. Tech. Rept. 1-026, London Underground.

Milillo, P., Giardina, G., DeJong, M. J., Perissin, D. & Milillo, G. (2018). Multi-temporal InSAR structural health monitoring via Relative Stiffness Method: the London Crossrail case study. *Remote Sens.* **10**(2), 287.

Peck, R. (1969). Deep excavations and tunneling in soft ground. In *Proceedings of the 7th International Conference on Soil Mechanics and Foundation Engineering*, Mexico City, pp. 225–290.

Potts, D. M. & Addenbrooke, T. I. (1997). A structure's influence on tunnelling-induced ground movements. *Proceedings of the Institution of Civil Engineers: Geotechnical Engineering* **125(**2), 109–125.

Son, M. & Cording, E. J. (2005). Estimation of building damage due to excavation-induced ground movements. *Journal of Geotechnical and Geoenvironmental Engineering* **131**(2), 162–177.

Torp-Petersen, G. & Black, M. (2001). Geotechnical investigation and assessment of potential building damage arising from ground movements: Crossrail. *Proceedings of the Institution of Civil Engineers – Transport* **147(**2), 107–119.

Accepted manuscript doi:
10.1680/jgeen.18.00178

Table 1. Selected case study key parameters.

Case Study	Building Width B (m)	Building Length L (m)	Building Height H (m)	Average Tunnel Depth z_0 (m)	Bending Stiffness EI (Nm^2)	Axial Stiffness EA (N)	Reference soil stiffness E_s (MPa)
129-133 Park Lane	14.7	44.0	21	33.7	4.1×10^{10}	1.0×10^{9}	177.2
6-14 Bedford Row	41.1	77.5	16	29.5	2.1×10^{10}	4.4×10^{8}	143.9
172-184 Shaftsbury Avenue	20.5	59.0	20	19.4	2.6×10^{10}	6.9×10^{8}	99.8
39-44 Berwick Street	21.2	39.8	16	25.0	1.3×10^{10}	5.4×10^{8}	124.5

Accepted manuscript doi:
10.1680/jgeen.18.00178

Table 2. Predicted deflection ratios (Δ / L) and modification factors (M^{DR}) for the case studies

(a) Sagging					
Case Study	**Greenfield**	**Potts and Addenbrooke (1997)**	**Franzius (2006)**	**Goh and Mair (2011) Lower Bound**	**Goh and Mair (2011) Upper Bound**
	$(\Delta / L)^{g}_{\text{sag}}$	$M^{DR,\text{sag}}$	$M^{DR,\text{sag}}$	$M^{DR,\text{sag}}$	$M^{DR,\text{sag}}$
129-133 Park Lane	2.76×10^{-6}	0.04	0.26	N/A	N/A
6-14 Bedford Row	2.22×10^{-4}	1.02	1.11	0.4	1
172-184 Shaftsbury Avenue	3.37×10^{-4}	0.69	0.85	0.03	0.59
39-44 Berwick Street	1.71×10^{-4}	0.77	1.19	0.21	0.81

(b) Hogging					
Case Study	**Greenfield**	**Potts and Addenbrooke (1997)**	**Franzius (2006)**	**Goh and Mair (2011) Lower Bound**	**Goh and Mair (2011) Upper Bound**
	$(\Delta / L)^{g}_{\text{hog}}$	$M^{DR,\text{hog}}$	$M^{DR,\text{hog}}$	$M^{DR,\text{hog}}$	$M^{DR,\text{hog}}$
129-133 Park Lane	3.42×10^{-5}	0.81	1.27	0.05	0.63
6-14 Bedford Row	7.72×10^{-5}	0.92	1.28	0.17	0.77
172-184 Shaftsbury Avenue	1.15×10^{-4}	0.47	1.08	0.00	0.39
39-44 Berwick Street	6.47×10^{-5}	0.24	0.89	0.00	0.42

Accepted manuscript doi:
10.1680/jgeen.18.00178

Figure captions

Figure 1. Location plan of 129-133 Park Lane (shaded in red) with predicted settlement contours.

Figure 2. (a) Image of Nos. 129-131 Park Lane (129 Park Lane is closest to the street corner); (b) image of Avenfield House, just south of 129-131 Park Lane (Google Streetview).

Figure 3. Plan view of building and monitoring locations (a) and transect elevation view of measured settlement values (b) for 129-133 Park Lane.

Figure 4. Location plan for 6-14 Bedford Row (shaded in red) with predicted settlement contours.

Figure 5. Google Streetview of Bedford Row terrace.

Figure 6. Plan view of building and monitoring locations (a) and transect elevation view of measured settlement values (b) for 6-14 Bedford Row.

Figure 7. Location plan for 172-184 Shaftesbury Avenue (shaded in red). The eastbound tunnel is shown in red and travels directly beneath 172-176 Shaftesbury Avenue.

Figure 8. Google Streetview Image: 172-184 Shaftesbury Avenue.

Figure 9. Plan view of building and monitoring locations (a) and transect elevation view of measured settlement values (b) for 172-184 Shaftsbury Avenue.

Figure 10. Location plan for 38-44 Berwick Street (shaded in red) with predicted settlement contours.

Figure 11. Google Streetview of Berwick Street, with 44 Berwick Street on the left.

Figure 12. Plan view of building and monitoring locations (a) and transect elevation view of measured settlement values (b) for 38-44 Berwick Street.

Figure 13. Google Streetview looking towards the west side of Wardour Street, just north of D'Arblay Street.

Figure 14. Deflection ratio in sagging and hogging zone (after Franzius et al. (2006))

Figure 15. Results of the RSM application to the case studies.

Accepted manuscript doi:
10.1680/jgeen.18.00178

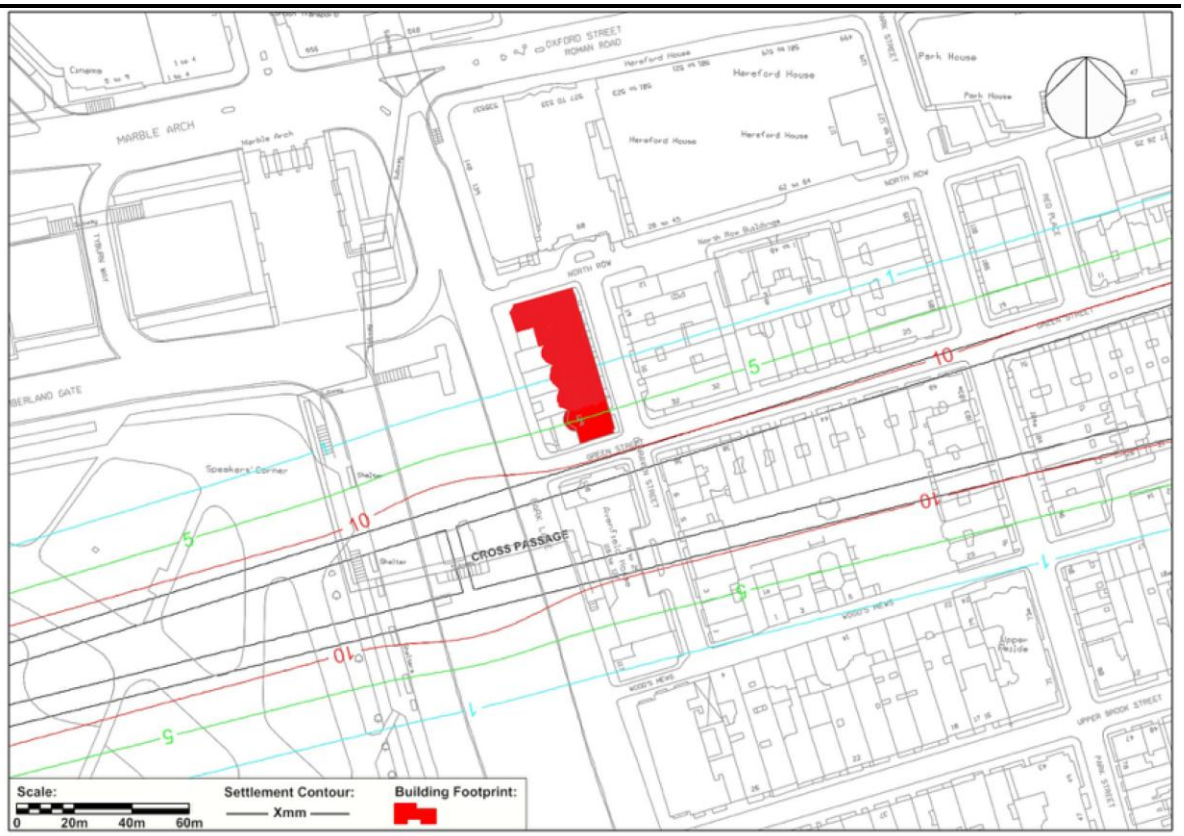

Fig. 1.

Accepted manuscript doi:
10.1680/jgeen.18.00178

(a) (b)

Fig. 2.

Accepted manuscript doi:
10.1680/jgeen.18.00178

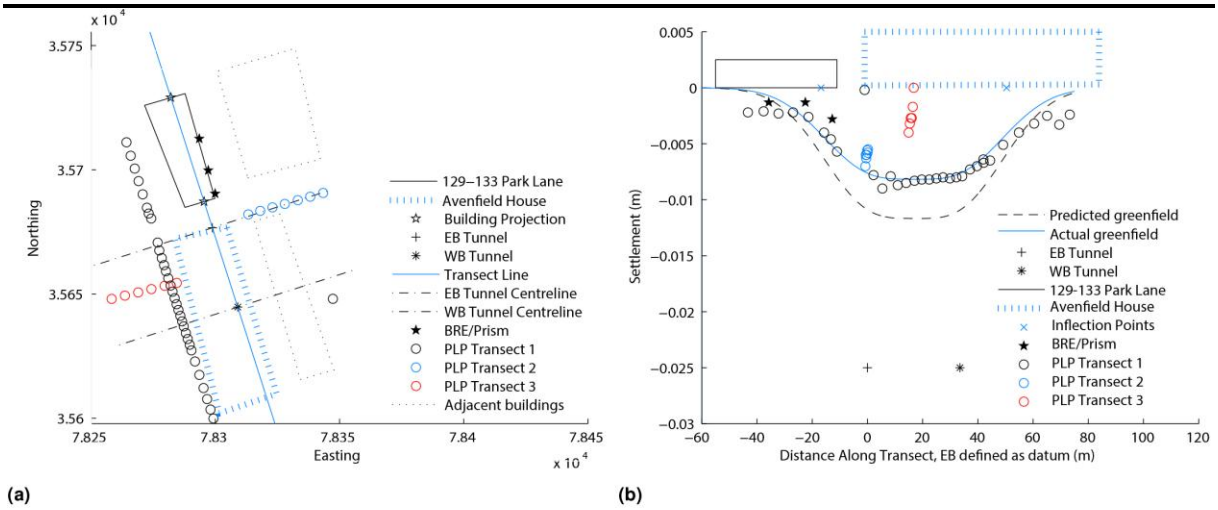

Fig. 3

Accepted manuscript doi:
10.1680/jgeen.18.00178

Fig. 4.

Accepted manuscript doi:
10.1680/jgeen.18.00178

Fig. 5.

Accepted manuscript doi:
10.1680/jgeen.18.00178

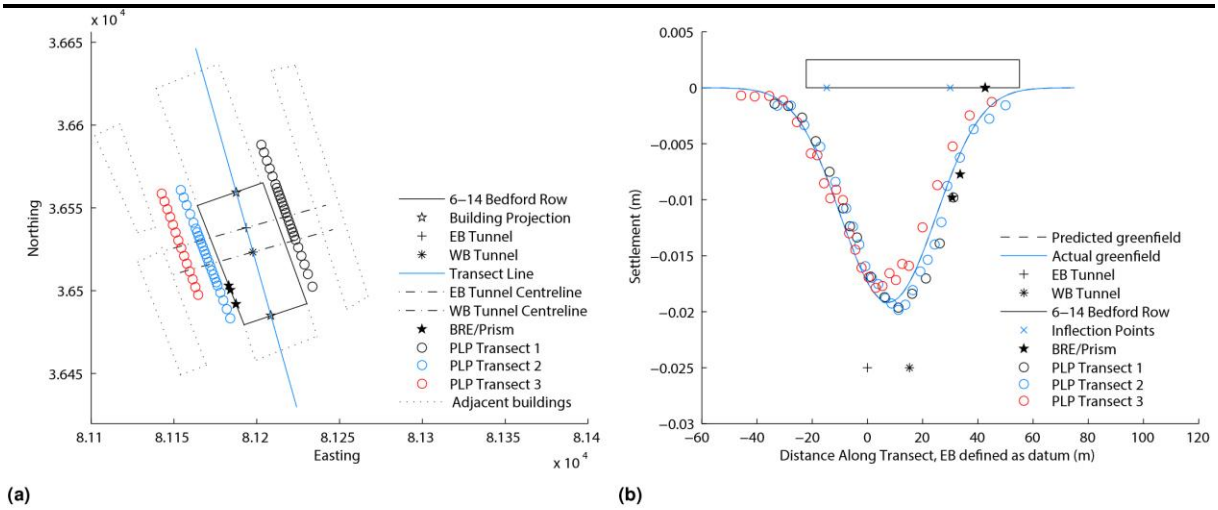

Fig. 6

Accepted manuscript doi:
10.1680/jgeen.18.00178

Fig. 7.

Accepted manuscript doi:
10.1680/jgeen.18.00178

Fig. 8

Accepted manuscript doi:
10.1680/jgeen.18.00178

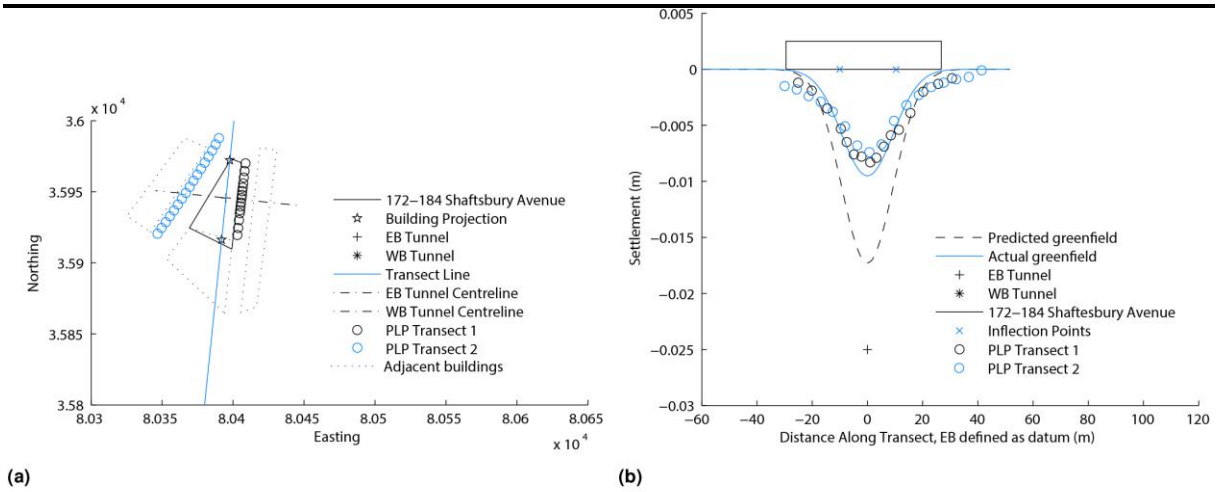

(a) (b)

Fig. 9.

Accepted manuscript doi:
10.1680/jgeen.18.00178

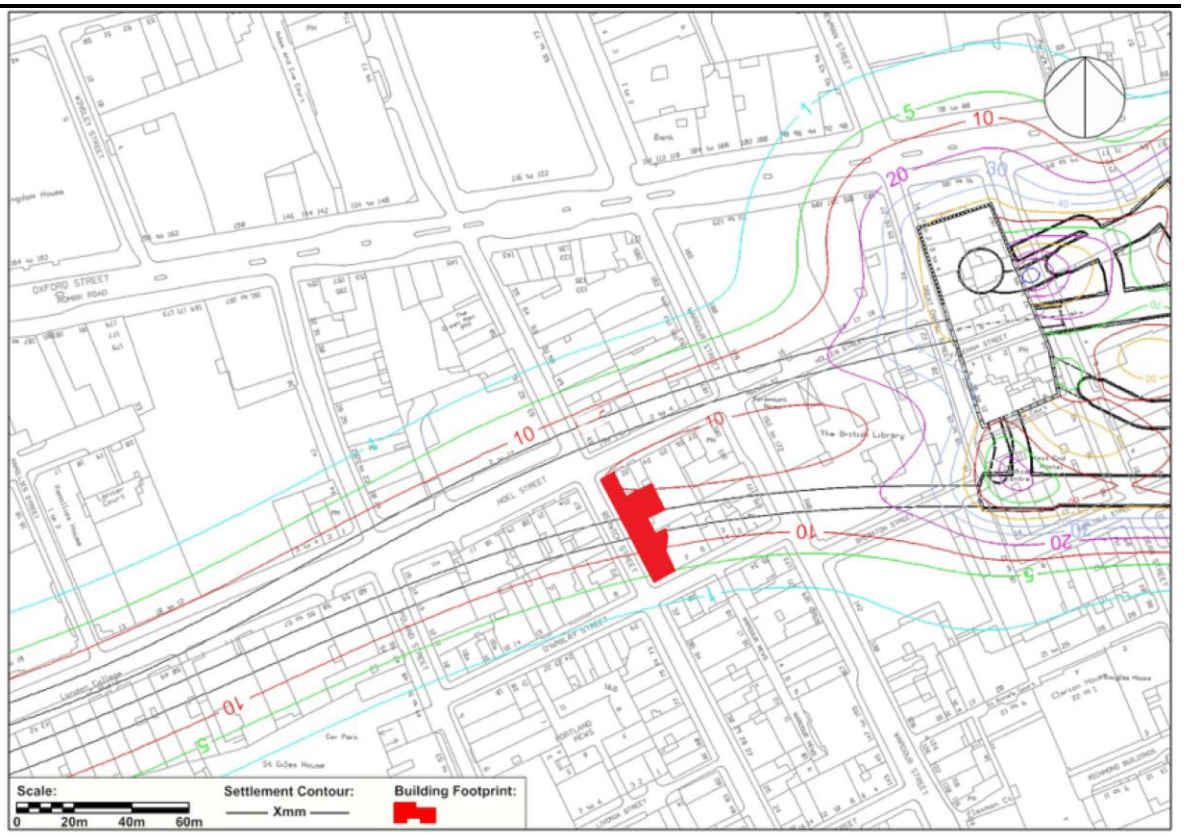

Fig. 10.

Accepted manuscript doi:
10.1680/jgeen.18.00178

Fig. 11.

Accepted manuscript doi:
10.1680/jgeen.18.00178

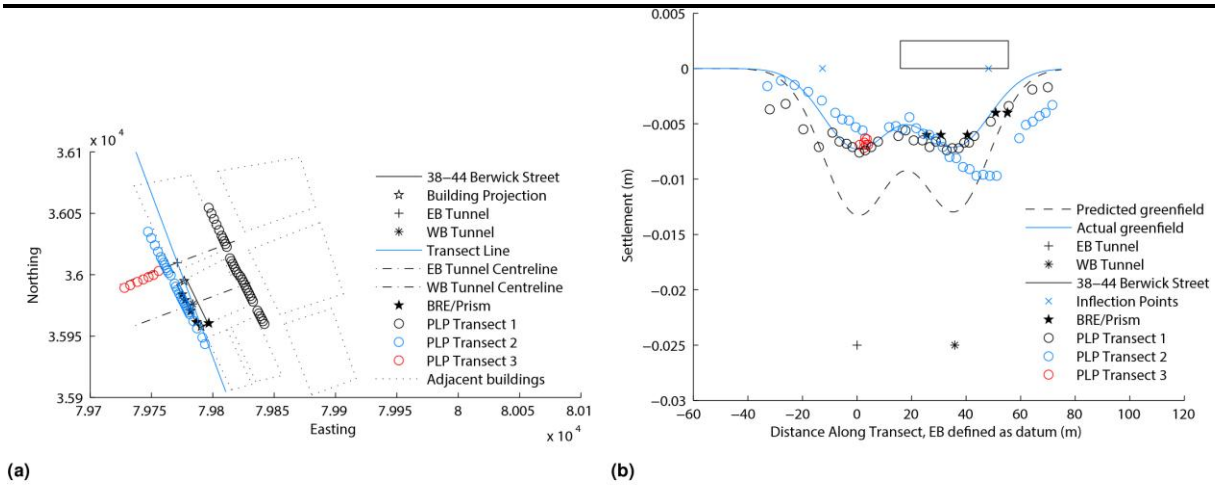

Fig. 12.

Accepted manuscript doi:
10.1680/jgeen.18.00178

Fig. 13.

Accepted manuscript doi:
10.1680/jgeen.18.00178

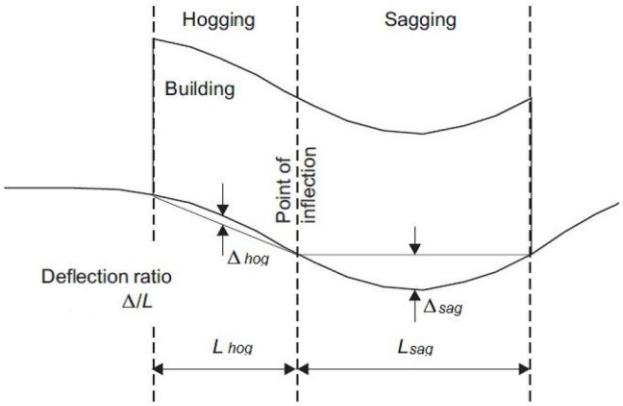

Fig. 14.

Accepted manuscript doi:
10.1680/jgeen.18.00178

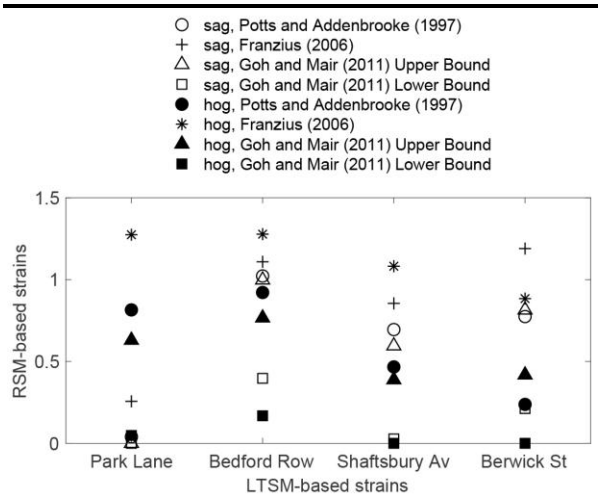

(a) Predicted modification factors

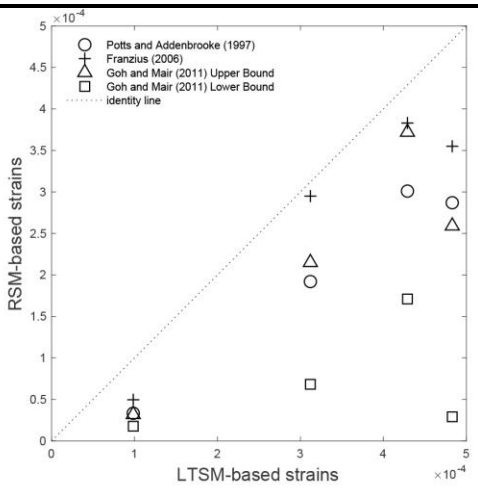

(b) Comparison between total strains from the LTSM and from the RSMs

Fig. 15.